Cerebral Cortex Advance Access published September 7, 2013

Cerebral Cortex
doi:10.1093/cercor/bht231

Cortical and Subcortical Connections of the Human Claustrum Revealed In Vivo by Constrained Spherical Deconvolution Tractography

Demetrio Milardi[1,4], Placido Bramanti[4], Carmelo Milazzo[1], Giovanni Finocchio[2], Alessandro Arrigo[1], Giuseppe Santoro[1,4], Fabio Trimarchi[1,4], Angelo Quartarone[2,3], Giuseppe Anastasi[1,4] and Michele Gaeta[1,4]

[1]Department of Biomedical Sciences and Morphological and Functional Imaging, [2]Department Electronic Engineering, Chemistry and Industrial Engineering, [3]Department of Neurosciences, University of Messina, Messina, Italy and [4]IRCCS Centro Neurolesi Bonino Pulejo, Messina, Italy

Address correspondence to Angelo Quartarone, Department of Neurosciences, University of Messina, Via Consolare Valeria 1, Messina 98125, Italy. Email: angelo.quartarone@unime.it

The claustrum is a thin layer of gray matter that is at the center of an active scientific debate. Recently, Constrained Spherical Deconvolution (CSD) tractography has proved to be an extraordinary tool allowing to track white matter fibers from cortex to cortical and subcortical targets with subvoxel resolution. The aim of this study was to evaluate claustral connectivity in the human brain. Ten normal brains were analyzed by using the High Angular Resolution Diffusion Imaging CSD-based technique. Tractography revealed 4 groups of white matter fibers connecting the claustrum with the brain cortex: Anterior, posterior, superior, and lateral. The anterior and posterior cortico-claustral tracts connected the claustrum to prefrontal cortex and visual areas. The superior tract linked the claustrum with sensory-motor areas, while the lateral pathway connected the claustrum to the auditory cortex. In addition, we demonstrated a claustral medial pathway connecting the claustrum with the basal ganglia, specifically with caudate nucleus, putamen, and globus pallidus. An interesting and exciting new finding was the demonstration of a bilateral connection between claustrum and contralateral cortical areas and a well-represented interclaustral communication with interconnection bundles interspersed within the bulk of the trunk of the corpus callosum. The physiological and pathophysiological relevance of these findings are discussed.

Keywords: basal ganglia, claustrum, constrained spherical deconvolution, tractography

Introduction

The claustrum is a thin layer of gray matter, placed in the deep part of both the cerebral lobes, found in mammalian brains. Laterally, it is separated from the insular cortex by the extreme capsule and, medially, from the lenticular nucleus by the external capsule.

Due to the claustrum's location, size, and shape, it is very difficult to investigate its connections and functions even using the most sophisticated techniques that are currently available. Therefore, the detailed structure and function of claustrum remain enigmatic, consistent with the latin derivation of its name meaning "hidden place."

Recently, a high definition diffusion magnetic resonance imaging (MRI) study performed in the brain of prosimian primates (*Microcebus murinus*) has reported that claustrum exhibits a reciprocal widely distributed anatomical projections to almost all regions of the cortex and to many subcortical structures that are not passing through the thalamus (Park et al. 2012). This is in keeping with previous data on macaque monkeys, showing that the claustrum has extensive connections with the frontal, premotor, ventral anterior cingulate, ventral temporal, visual, motor, somatosensory, olfactory cortices, and more strongly with the entorhinal cortex (Tanné-Gariépy et al. 2002; Edelstein and Denaro 2004). Overall, these data suggest that claustrum can be broadly divided into 3 compartments: An antero-dorsal connected with the somatosensory and motor cortices, a posterior dorsal (visual cortex), and a ventral area (auditory cortex) (LeVay and Sherk 1981; Sherk and LeVay 1981; Edelstein and Denaro 2004; Crick and Koch 2005). In addition, connections with the thalamus, the caudate nucleus, and the amygdala have also been found (LeVay and Sherk 1981; Arikuni and Kubota 1985; Jiménez-Castellanos and Reinoso-Suárez 1985; Amaral and Insausti 1992; Edelstein and Denaro 2004).

Given these dense anatomical connections, the claustrum is not just a sort of shadow of the cortex, but rather a crucial node of a complex neural circuit with overlapping inputs from various cortical regions and outputs back to the cortex. Due to its widespread connections, Crick and Koch (2005) compared the claustrum to a conductor of an orchestra, who is responsible for binding the performances by individual musicians into an integrated whole that is much more than the sum of the parts. In other words, the claustrum acts as an integrator of synchrony binding together the various disparate components of the conscious experience represented in many different brain regions (Stevens 2005).

In a recent study, Fernández-Miranda et al. (2008) used the fiber dissection technique in combination with the diffusion tensor imaging (DTI) technique to evaluate claustro-cortical connections in humans. However, the fiber dissection technique is limited because of the complex relationships of the fiber systems, so that the demonstration of one fiber system often results in the destruction of other fiber systems (Ture et al. 2000). This issue can be effectively solved by Constrained Spherical Deconvolution (CSD) tractography, which can show the complex relationships between the fiber systems.

The aim of the present study is to demonstrate "in vivo" cortico-claustral connections, as well as the connections of the claustrum with subcortical gray matter in normal human subjects, by using CSD tractography.

Materials and Methods

Participants

The study was approved by our Ethical Committee and written informed consent was obtained from all subjects before MRI examination. A total of 10 human subjects (5 females and 5 males; mean age 32.1; age range 25–50 year) were recruited. All the participants were

right-handed, as confirmed by the Edinburgh Inventory (Oldfield 1971). No patient had a history of any overt neurological disease.

Data Acquisition

The study was performed with a 3-T Achieva Philips scanner; using a 32-channel SENSE head coil. In each patient, the following MRI sequences were carried out:

1. for anatomical comparison, a 3-dimensional (3D) high-resolution, T_1-weighted fast field echo (FFE) sequence was acquired using the following parameters: Repetition time 25 ms; echo time 4.6 ms; flip angle 30°; field of view (FOV) 240 × 240 mm^2; reconstruction matrix 256 × 256; voxel size 1 × 1 × 1 mm; slice thickness 1 mm. The acquisition time was 6 min;
2. diffusion MRI was acquired with a dual phase-encoded pulsed-gradient spin-echo sequence. Such sequence was chosen in order to improve the correction of susceptibility and Eddy's currents distortion (Embleton et al. 2010). The model used 60 gradient diffusion directions according to an electrostatic repulsion model (Jones et al. 1999).

The other sequence parameters were: Diffusion weighting *b*-factor 1200 s/mm^2; repetition time 11 884 ms; echo time 54 ms; FOV 240 × 240 mm^2; scan matrix 112 × 112; reconstruction matrix 256 × 256; axial slice thickness 2 mm; and no interslice gap. The sequence was repeated 4 times for each patient to correct subject motion and induced Eddy currents. An appropriate modulation of the diffusion-weighted (DW) images with the Jacobian of the transformation matrix (Jones and Cercignani 2010) was performed adjusting B-matrix (Leemans and Jones 2009). The total acquisition time was 25 min.

Higher *b*-values allow to obtain smaller angles among fibers (Alexander and Barker 2005; Behrens et al. 2007; Tournier et al. 2007), but increase acquisition time and make more difficult the correction of the motion and the Eddy currents. Thus, we preferred to use lower *b*-value in order to minimize these problems, keeping a feasible acquisition time.

Claustrum Segmentation and Tractography

We used a modified High Angular Resolution Diffusion Imaging (HARDI) technique, called non-negativity CSD. This technique estimates the fiber Orientation Distribution Function (fODF) directly from the DW signal by means of positive (avoiding the unreal negative regions) spherical deconvolution (Tournier et al. 2007). Spherical Harmonic degree was fixed equal to 8 in order to obtain robustness to noise.

The fODF is obtained by deconvolution of single fiber DW signal response and finding the components with specific orientation.

Using a method based on CSD to perform the extraction of local fiber orientations, we managed to overcome partial volume effects associated with DTI and also to improve, comparing with other types of HARDI acquisitions, the poor angular resolution achieved with QBI (Q-balls Imaging) discarding diffusion spectrum imaging (DSI) due to its longer acquisition time (Tournier et al. 2008).

We reconstructed a color-coded map in which red, blue, and green colors indicate the principal eigenvector's directions (Pajevic and Pierpaoli 1999). Specifically, the red color indicates a left–right pattern, the green color an anterior–posterior pattern, and the blue color a caudal–cranial pattern. Intensity and pureness of these colors vary according to the behavior of fibers in all intermediate positions.

Once recognized the claustra and the basal ganglia, regions of interest (ROIs) were manually defined to "filter in" the tracks crossing the regions.

Claustrum segmentation was manually performed by an experienced neuroradiologist using Analyze 11.0 (AnalyzeDirect, Inc.; Kansas City, Kansas, USA) as follows: First, the individual volumes obtained from the 3D T_1-weighted FFE sequence were loaded into the viewer; secondly, the contrast values in the viewer were set to maximally increase visibility of the nuclei; thirdly, the axial view was zoomed to facilitate the drawing of the claustrum mask. For each participant, the volumes of both claustra were estimated. Furthermore, the dataset acquired in 3 days of distance from 3 participants (6 claustra) was used to assess the reproducibility of segmentations (intraobserver variability), calculating the mean agreement index (AI) computed as $AI = 1 - [|V1 + V3|/(0.5 \times (V1 + V3))]$, where $V1$ and $V3$ are the measured volumes on days 1 and 3. On 3D images, volumes of interests (VOIs) were automatically reconstructed from ROI's. However, it is fair to recognize that the VOI reconstruction causes an apparent enlargement of the size of the subcortical nuclei, due to prospective representation of 3D structures on 2D images.

A further improvement in the definition of the fiber tracking was obtained by an anatomical model-based approach using regions of avoidance (ROAs) that, on the contrary, "filter out" the tracks (Verstynen et al. 2011). Multiple ROIs and ROAs were combined to fulfill the complicated tracking demand for each fiber bundle reconstruction.

To further improve the results obtained with CSD probabilistic tractography algorithm, we also used a bootstrap model in order to estimate a new fODF that accounts for uncertainty of the data (Cohen-Adad et al. 2011).

We managed the bias due to the uncertainty related to DW acquisition, estimating true population data variance through a Repetition Bootstrap Jacknife Realization (RBJR) model (Efron 1992). The use of such model allows both good confidence interval estimate and, using only a few number of acquisitions, probabilistic tractography without making assumptions about the sources of uncertainty in the data. By extracting the peaks with RBJR, we define a new fODF, sharper than the original (Chung et al. 2006).

From same seed points we traced, for each of 4 RBJR model repetitions, a generated dataset. From these results, we built the so-called "visitation maps" counting for each voxel the number of modelled trajectories passing through it (Bürger et al. 2012) .We performed probabilistic streamline fiber tracking evaluating fODF peak direction closest to the previous stepping direction (as stated by Newton's method in optimization) using trilinear interpolation.

The tracking is stopped when exists one of the following conditions doing streamline algorithm between 2 consecutive points: Step size = 0.2 mm, maximum angle = 10°, minimal fODF amplitude = 0.15 (this is a more conservative choice with respect to usual standards, since we preferred to underestimate fibers bundles in order to have consistent reconstruction without false positive) (Descoteaux et al. 2009; Tournier et al. 2011) or length fiber constraint of ≤100 mm (to include supposed interclaustral connections).

Axonal projections were traced in both anterograde and retrograde directions. Intersubject variability of the claustrum connections with Broadmann areas was evaluated, but no attempt was made to assess asymmetry of white matter tracts of the claustrum connectome.

All calculations were made by using the Matlab software (The MathWorks, Inc., USA) and validated with ExploreDTI tools (Leemans et al. 2009).

To identify the cortical Brodmann areas connected to the claustrum, we coregistered participants' brains on the Talairach Brain Atlas using 12 degrees of freedom registration algorithm.

Results

We detected 4 groups of white matter fibers connecting claustrum to the cortex: Anterior, posterior, superior, and lateral.

The anterior and posterior cortico-claustral tracts were well visible on sagittal view (Fig. 1*a*,*b*). They appeared green due to their anterior and posterior directions. After the coregistration on the Talairach Atlas, we found that connected brain areas were for the anterior and posterior pathways 11, 12, 10, 9 (prefrontal cortex), 8, 34 (anterior entorhinal cortex), 17 (primary visual cortex), 18, 19, and 39, respectively. At the level of the anterior part of the external capsule, the anterior pathway is located in close relationship with uncinate, inferior fronto-occipital, and inferior longitudinal fasciculi (Fig. 2).

The superior pathway appeared as a large fan of fibers that reached parietal and frontal cortical areas 8, 6, 4 (primary motor cortex), 3, 1, 2 (primary somatosensory cortex), 5, and 7

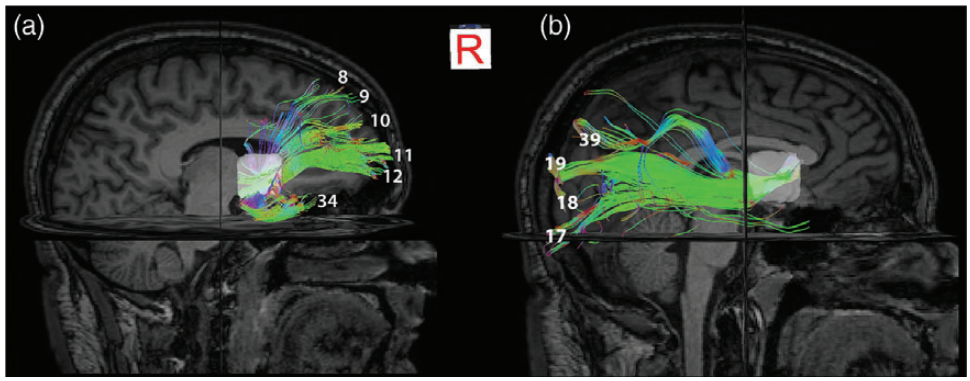

Figure 1. Sagittal view of the anterior (*a*) and posterior (*b*) cortico-claustral pathways. The prevalent color (green) indicates that the orientation of the fibers was antero-posterior. Brodmann areas reached by the pathways are also shown.

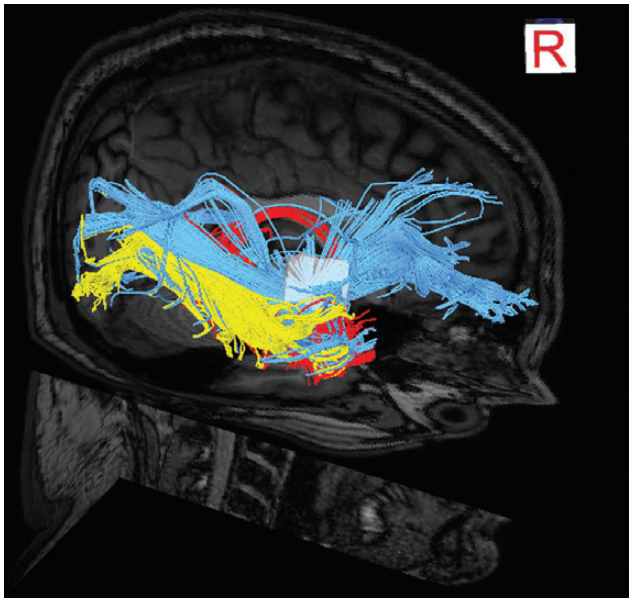

Figure 2. The close relationship between anterior and posterior cortico-claustral pathways (light blue color), uncinate fasciculum (red color), and inferior longitudinal fasciculum (yellow) is well depicted on the lateral view. Note that colors in this figure do not show the direction of the white matter fibers, but are used to differentiate the different fascicula.

with a predominant cranio-caudal direction, as shown in Figure 3. On the color map, they appeared predominantly blue at their origin; however, large components of fibers turned to green and red-blue for the presence of bundles which changed direction along their upper course.

The various bundles of the lateral pathway, for their complex 3D spatial disposition, were difficult to be distinguished and needed of both sagittal and axial views to be well depicted (Fig. 4*a*,*b*), as red color tracts due to their medial–lateral direction. On the sagittal view (Fig. 4*b*), the connected brain areas 39, 31, 22, 41, and 42 (auditory cortex), 43, 44, and 45 were indicated.

The cortico-claustral fibers ran mainly within the external capsule and superiorly entered the corona radiata at the superior edge of the putamen (Fig. 5*c*).

Outside the cortex, we demonstrated the claustral medial pathway connecting the claustrum with the basal ganglia, specifically with caudate nucleus, putamen and globus pallidus (Fig. 5).

In addition, we found connections between the claustrum and the contralateral brain hemisphere, which occurred along 2 pathways: Cortico-claustral (Fig. 6*a*,*b*) and interclaustral (Fig. 7*a*,*b*).

Interhemispheric cortico-claustral fibers originated from the superior claustrum and crossed the corpus callosum reaching areas 6 (premotor cortex and supplementary motor cortex), 8, and 9 of the contralateral hemisphere (Fig. 6*b*).

The interclaustral connection consisted of small axonal contingents passing mainly through the anterior part of the trunk of the corpus callosum interspersed within the bulk of interhemispheric fibers (Fig. 7*b*). They entered both the dorsal and ventral claustrum without topographic distribution.

The whole interhemispheric connectome of the claustrum appears as a well-represented network of white matter tracts (Fig. 8).

In each of 10 examined brains, all the described pathways were seen. However, in 2 patients, we were not able to demonstrate, on the right side, the connections of the superior and posterior pathways with areas 19 and 5, respectively. It could be hypothesized that these differences were due to the well-known intersubject variability of white matter tracts. Indeed, a variability of cortico-spinal tracts, optic radiations, uncinate fasciculus, and inferior fronto-occipital fasciculus have been reported in both postmortem anatomical studies and in vivo tractography (Highley et al. 2002; Thiebaut de Schotten et al. 2011).

In addition, we cannot exclude that this variability could be related to an error introduced by the use of Tailarach brain atlas for coregistration of images for all the subjects. It is well known that every brain atlas, despite totally accepted by scientific community, can cause errors. This is the consequence of the method used to obtain atlas datasets as a mathematical average of brains (Laird et al. 2010)

It is worthy to note that the use of navigated transcranial magnetic stimulation, in combination with tractography, could improve the analysis of the white matter connections (Milazzo et al. 2012).

Table 1 summarizes our data, in comparison also with data obtained in monkeys. In the same table, the functions of human brain regions connected with the claustrum are highlighted.

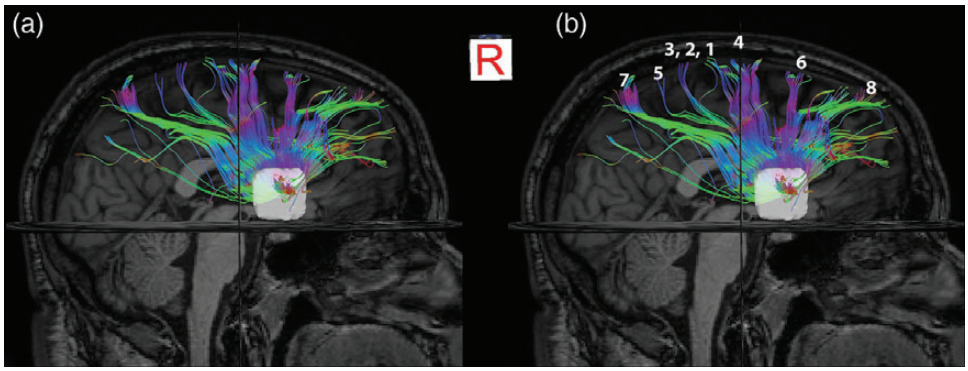

Figure 3. Sagittal view demonstrates the superior cortico-claustral pathway (*a*), as well as the connected Brodmann areas (*b*).

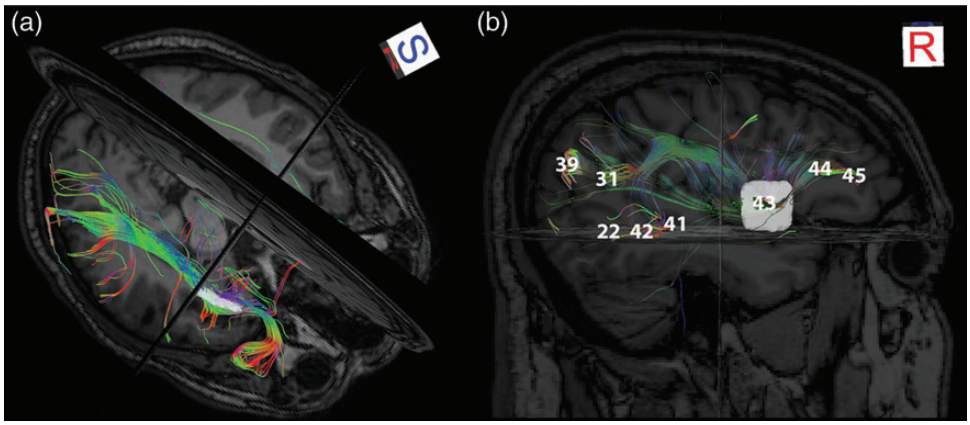

Figure 4. Axial oblique (*a*) and sagittal (*b*) views of the cortico-claustral lateral pathway. On the sagittal view (*b*), the Brodmann areas reached by the pathway are highlighted.

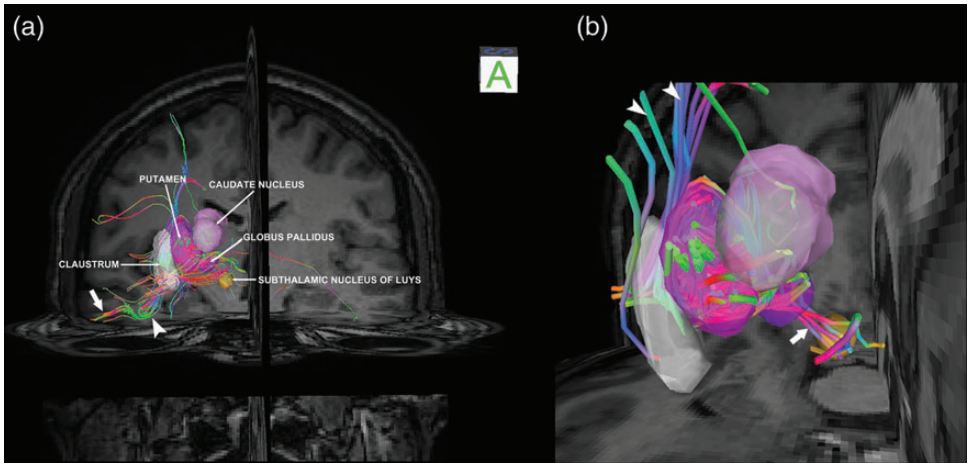

Figure 5. Coronal view shows the cortico-claustral medial pathway spreading between claustrum and basal ganglia (*a*). Note that also the fibers of the lateral pathway reaching the hippocampus (arrowhead) and the temporal cortex (arrow) can be clearly seen on the coronal view. An enlarged view focused on the medial pathway (*b*) shows the close relationship between the fibers and the basal ganglia with better advantage. Since the fibers spread in a complex 3D way, they appear green, red, and blue colored in different segments accordingly to their main changing direction. The fibers can be seen among translucent rendered VOIs. In addition, fibers of the superior claustral pathway are visible (arrowheads) passing mainly through the capsula externa. Note that CSD tractography permits to represent the connection (arrow) between globus pallidus and subthalamic nucleus of Luys, although this does not belong to the claustrum connectome.

Claustrum Volume

Concerning the reproducibility of the segmentation the AI was 0.90. Our intraobserver AI is of the same order of previous results on manual and automatic segmentation of brain structures (Joe et al. 1999; Babalola et al. 2009).

The mean volume was 813.6 mm^3 for the right claustrum (range 744–864) and 804.0 mm^3 for the left claustrum (range 752–912). The mean volume for all the 20 claustra was 808.8 mm^3.

In males, the mean volume was 835.2 mm^3 for the right claustrum, and 822.4 for the left claustrum (mean 828.8 mm^3);

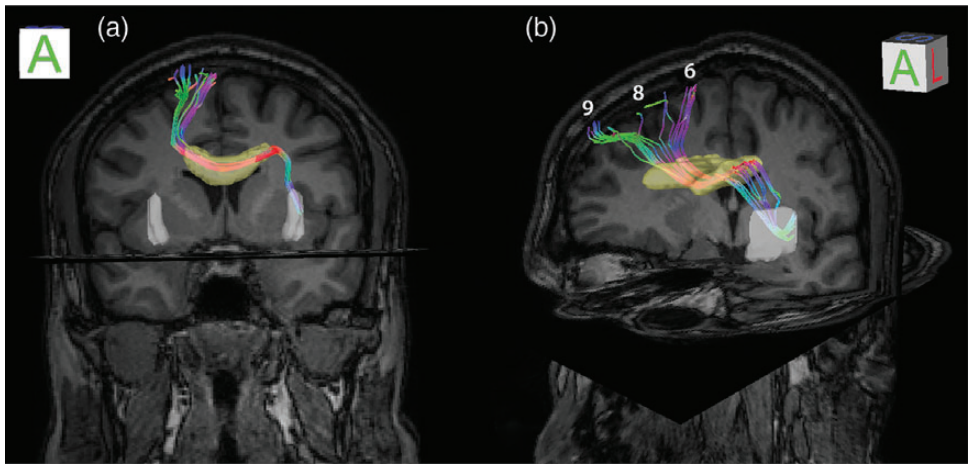

Figure 6. Coronal view (*a*) shows the pathway between left claustrum (white VOI) and contralateral cortical brain passing through the trunk of the corpus callosum (translucent yellow VOI). Oblique coronal view (*b*) allows to detect with better advantage the cortical areas reached by the pathway.

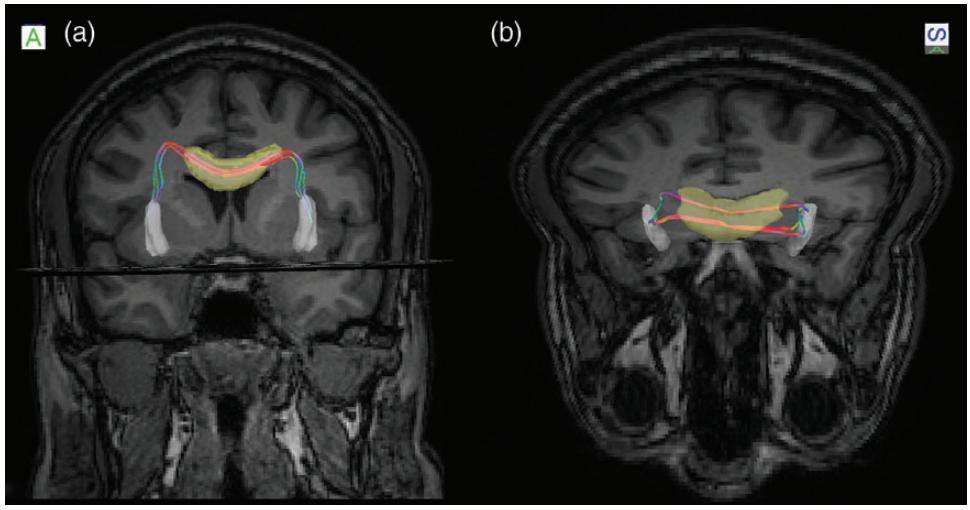

Figure 7. Coronal (*a*) and axial (*b*) views of the interclaustral connectivity. The axial view (*b*) shows with better advantage that the interclaustral contingent is prevalently located in the anterior part of the trunk of the corpus callosum (translucent yellow VOI). Claustra are shown as white VOIs.

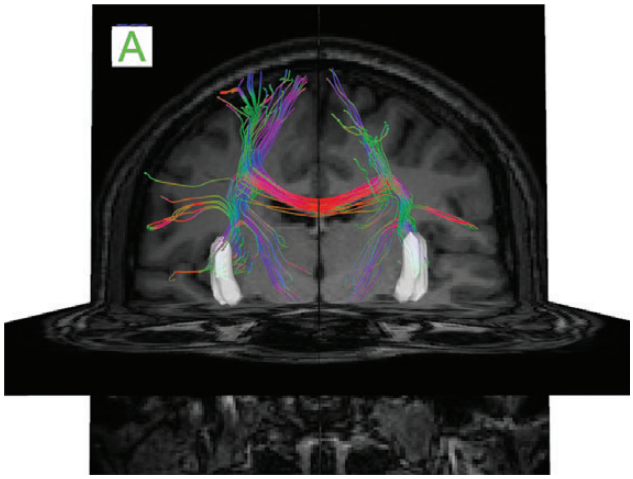

Figure 8. The whole interhemispheric claustrum connectome is showed on this figure. Some fibers of the medial and lateral pathways are visible.

in females, the mean volumes were 792.0 and 785.6 mm^3 for the right and left claustrum, respectively (mean 788.8 mm^3).

Statistical differences were evaluated using 2-tailed *t*-test; *P* values of <0.05 were considered to indicate statistically significant differences. Differences of the claustrum volumes between the left and right side as well as between males and females were not statistically significant ($P > 0.005$).

Discussion

By using in vivo DSI tractography, we demonstrated that, in normal humans, claustrum has a widely distributed anatomical network to almost all regions of the cortex as well as to many subcortical structures.

In particular, tractography reconstruction revealed 4 groups of white matter bundles connecting the claustrum with the brain cortex: Anterior, posterior, superior, and lateral.

The anterior and posterior cortico-claustral tracts were well visible on sagittal view connecting the claustrum to 12, 11, 10, 9, 8, and 34 and 17, 18, 19, and 39 Brodmann areas, respectively.

Table 1
Comparison between our findings in the human brain and other results in the animal brain with the anatomical and functional correspondences of Brodmann's areas involved

Monkey	Human brain (HDFT results)	Human functional correspondences
Frontal cortex, prefrontal cortex	Orbitofrontal areas (11, 12)	Executive function, cognitive control
	Premotor area (8, 9, 10)	Executive function, cognitive control
	Supplementary motor area (6)	Sensory guidance of movement
	Primary motor area (4)	Control of voluntary movements
Somatosensory cortices	Primary somatosensitive area (3, 2, 1)	Basic somatosensory functions
	Secundary somatosensitive areas (5, 7)	Visuo-motor coordination and elaboration of mechanoceptors and proprioreceptors of body
Parietal cortex	Primary and associative auditory areas (41, 42)	Auditory elaboration
Occipital cortex	Visual areas (17, 18, 19)	Visual elaboration
Temporal cortex	Wernicke's area (22, 39)	Language comprehension
	Broca's area (43, 44, 45)	Language production
Limbic cortex	Limbic area (34)	Memory and learning
Cingulate gyrus	Cingulate gyrus (31)	Emotion processing and recognition
Caudate nucleus, putamen, globus pallidus	Caudate nucleus, putamen, globus pallidus	Motor control
–	Corpus callosum	Interhemispheric connection

The superior tract appeared as a large fan of fibers reaching the parietal and frontal cortical areas namely 8, 6, 4, 3, 2, 1, 5, and 7 with a predominant cranio-caudal direction.

Finally, bundles of the lateral pathway connected the claustrum with brain areas 39, 31, 22, 42, 41, 43, 44, and 45.

These data are in keeping with several anatomic and functional studies obtained on different animal species. For instance, the claustrum of the cat was found to have a discrete visual and somatosensory fiber subdivisions interconnected with the corresponding brain areas. These areas have claustral retinotopic and somatotopic organization (Levay and Sherk 1981; Smiley and Falchier 2009). It was also seen the presence of a similar auditory organization (Olson and Graybiel 1980).

Moreover, our data are also in keeping with several neuroanatomical studies in monkey that have revealed widespread interconnections between the claustrum and most allocortical and neocortical regions, particularly within the frontal lobe, including motor, prefrontal, and cingulate cortices (Tanné-Gariépy et al. 2002).

Outside the cortex, we demonstrated a claustral medial pathway connecting the claustrum with the basal ganglia (caudate nucleus, putamen, and globus pallidus) (Arikuni and Kubota 1985).

In addition, in accordance with previous studies, we demonstrated that claustrum is also interconnected with prepiriform olfactory cortex and the entorhinal cortex; and also projects to the hippocampus (Amaral and Cowan 1980) and the amygdala (Amaral and Insausti 1992).

Despite the relatively large number of studies on the anatomy of claustrum in different animal species, there is only one report available in humans (Fernández-Miranda et al. 2008).

In a study, using the fiber dissection technique and DT imaging-based tractography, Fernández-Miranda et al. (2008) revealed the presence of an extensive, intricate claustro-cortical system. In particular, they showed that the claustro-cortical fibers connected the dorsal claustrum with the superior frontal, precentral, postcentral, and posterior parietal cortices with a rigid topographic organization.

In addition, they showed that the ventral part of the claustrum is connected with the orbitofrontal, prefrontal, and temporal cortex and with the amygdala.

However, in comparison with the work of Fernández-Miranda et al. (2008), our approach provided a more detailed representation of brain areas connected to the claustrum according to the Brodmann map.

Although Fernández-Miranda et al. (2008) demonstrated, by microsurgical dissection, a close relationship between the claustrum and other subcortical structures, such as basal ganglia and the limbic system (amygdala and prepiriform cortex), they did not obtain a tractographic demonstration of these connections. On the contrary, in our experience, by using CSD tractography, we could track a claustral medial pathway connecting the claustrum with caudate nucleus, globus pallidus, putamen, and hippocampal region (Figs 2*a* and 5).

Particularly interesting, as an extension of the findings of Fernández-Miranda et al. (2008), we could also demonstrate the existence of bilateral connections between claustrum and contralateral cortical areas and a well-represented interclaustral bundle passing through the trunk of the corpus callosum.

To our knowledge, no previous description of such interhemispheric claustral connectivity has ever been reported in humans.

Interclaustral connections were described in rats along the claustrum rostro-caudal axis (Smith and Alloway 2010). These extensive intraclaustral connections are probably conceived for rapid interhemispheric transmission of information needed for bilateral coordination of the M1 regions regulating whisker movements (Smith and Alloway 2010). Moreover, a recent HARDI study performed on *M. murinus*, a prosimian primate, reported that the claustrum has cross-hemispheric connections via the anterior commissure and the corpus callosum, even though no detailed description of these fibers was made (Park et al. 2012).

As a further evidence for interclaustral cross-talking, in a PET study on brain processing of visual sexual stimuli in 9 healthy human males, Redouté et al. (2000) found activation in paralimbic areas (anterior cingulate gyrus and orbitofrontal-cortex), in striatum (head of caudate nucleus and putamen), in the posterior hypothalamus, and within the claustrum. A bilateral activation of the claustrum was one of the most striking findings. Since the brain processing of visual sexual stimuli has a critical sociobiological importance in human beings, this study is a further evidence of the involvement of the claustrum in multisensorial and motivational processes and confirms the presence of a relevant interclaustral functional and anatomical connection.

Although the connection between the claustrum and contralateral cortex has never been reported previously in the human brain, it was found in cats and rats (Norita 1977; Druga

1982) and, more important, in primates. In cats, stimulation of the claustrum influenced ipsi- and contalateral oculomotor neurons and complete section of the corpus callosum abolished the influence on the contralateral cortex, suggesting the existence of a direct claustro-contralateral oculomotor cortex pathway running through the corpus callosum (Cortimiglia et al. 1991). In addition, projections from the precentral motor cortex to the ipsi- and contralateral claustrum were demonstrated in 7 monkeys by tracing radioactively labeled proteins transported by axonal flow (Kunzle 1975). These data are strongly in keeping with our description of interhemispheric cortico-claustral pathways.

We also estimated claustra volume in all the participants. In our knowledge, only an other MRI study has been reported on this topic (Davis 2008).

Davis (2008), in 14 normal boys and in 16 boys with autism, found an average claustrum volume measured with MRI of 701 and 555 mm^3, respectively. In addition, using a 3D reconstruction in a cadaver, volumes of 828.8 and 705.8 mm^3 were found for the right and left claustrum, respectively (Kapakin 2011). These data are in keeping with our results.

We found that the right claustrum had a larger volume than the left one, but the difference was not significant. Other subcortical structures have also shown to exhibit hemispheric differences, such as the amygdala (right > left) (Pedraza et al. 2004) and the subthalamic nucleus (left > right) (Fortsmann et al. 2012). It is unclear why such laterality would exist; however, it has been reported that the right claustrum is more active than the left one during modal sensory integration of conceptually related objects (Naghavi et al. 2007) and suppression of natural urges (Lerner et al. 2009).

The knowledge of the normal range of claustrum volume could be potentially useful to detect early claustrum shrinkage due to neuronal loss in pathological conditions. For example, the smaller claustral volume found by Davis in individuals with autism is in keeping with the under-connectivity found in autism by Just et al. (2007), probably because the claustrum acts as an integrating center for all cortical modalities.

Physiological and Clinical Considerations

Functionally, the claustrum becomes active during cross-modal processing especially when integrating tactile and visual representations (Uhlhaas et al. 2009), being a substantial multimodal convergence zone within primates (Pearson et al. 1982)

In this way, during multimodal perceptual and cognitive operation, reverberating claustro-cortical circuits could integrate haptic, visual, auditory, and emotional representations (Smythies et al. 2012). In this regard, it has been postulated that claustrum is a key structure in the neural mechanisms implicated in consciousness (Stevens 2005). Indeed, a key feature of our conscious experiences is that all the components must be integrated into a unified whole: How a rose looks, smells, and feels are bound together with our emotional experience of it. As these different aspects of experience are conveyed by separate brain circuits (those responsible for vision, olfaction, somatic sensation, together with the amygdala, and other centers involved in emotion), this unification of experiential components implies a central node responsible for the coordination between those different brain areas (Crick and Koch 2005; Smythies et al. 2012). Giving the extensive connections of the claustrum with the entire brain, as shown in the present study, it is not surprising that an influent current view suggests that claustrum, like the thalamus, can play such a coordination role. In their seminal review on the physiology of claustrum, Crick and Koch (2005) compared the claustrum to an orchestra conductor coordinating a group of players (the various cortical regions). "Without the conductor, the players can still play but they fall increasingly out of synchrony with each other. The result is a cacophony of sounds." This metaphor would suggest that different attributes of a given object, both within (e.g., color and motion) and across modalities (e.g., visual form and sound location), are rapidly combined and bound into the claustrum (Crick and Koch 2005).

According to this view, imaging functional data suggest that the claustrum is activated to overcome a visuo-motor transformation during cross-modal processing, integrating haptic, and visual representation (Hadjikhani and Roland 1998; Calvert 2001; Baugh et al. 2011).

Taken together, the anatomy and functional activation of the claustrum has led to theories that the claustrum may play a substantial role in multisensory integrative processing (Molholm et al. 2002; Martuzzi et al. 2007).

The existence of a interhemispheric connections allows us to speculate that, in the human brain, claustra could be able to coordinate bilateral cortical functions by this interclaustral system of communication.

In addition, the claustrum could be involved in the process of "working memory" (Zhou et al. 2007) by means of its ispsilateral and contralateral connections with prefrontal, premotor, and motor areas. Future studies using fMRI are needed to clarify the physiological role of interhemispheric claustral fibers.

What happens when the claustrum or parts of it are transiently or permanently removed? The answer to this important question remains still unsolved.

As far as we know, there are no humans with claustrum agenesia. There are only few lesional studies available in humans, which can be helpful in understanding claustrum physiology. In an influent study, Duffau et al. (2007) showed the absence of permanent sensorimotor or cognitive disorders after unilateral resection of the claustrum in cases of insular gliomas. The presence of the interhemispheric claustral connections, as shown in the present study, could be the anatomical basis for the explanation of this compensatory phenomenon. On the other hand, selective bilateral lesions of the claustrum and external capsule have been reported in patients with herpes simplex encephalitis (Kimura et al. 1994) and anecdotally in Sugihiritake mushroom poisoning (Sperner et al. 1996; Nishizawa 2005). Interestingly in all the reported cases, patients developed a severe encephalopathy with disturbance of consciousness, seizures, and psychotic symptoms.

Claustral pathology has been described in Lewy Body Dementia (DLB; Kosaka 1978; Yamamoto et al. 2007) and is related to the presence of visual hallucinations, while in Alzheimer Disease (AD) is related to the presence of dementia and cognitive dysfunction (Morys et al. 1996). Considering the extensive connections of the claustrum with the frontal, temporal, entorhinal cortices and with the hippocampus, amygdala, caudate nucleus, and putamen, it is not difficult to envision a role of claustral pathology in the development of dementia in Parkinson Disease (PD) and DLB. Finally, in boys with autism, claustrum is significantly smaller than in normal boys (Davis 2008).

Further studies are necessary to evaluate cortical and subcortical connections of the claustrum in basal ganglia disorders using tractography and functional MRI.

Limitations

Due to the relatively small number of subjects included in the present study, we did not address the presence of asymmetry of white matter bundles between the 2 hemispheres. This is a limitation of the study considering that many white matter tracts such as cortico-spinal, optic radiations, and uncinate fasciculum show asymmetry (Highley et al. 2002; Thiebaut de Schotten et al. 2011).

A further drawback of our work is linked to the inherent limitation of the tractography. For example, reliability of tractography is usually not sufficient to evaluate properly the reconstructed pathways. However, we have minimized this limitation by using CSD and bootstrap combined methods. This approach can overcome most of the limitations except those related to low anisotropy crossing fibers (Parker et al. 2013).

In addition, the directionality (afferent–efferent) of the connections cannot be evaluated (Chung et al. 2011; Parker et al. 2013).

Another factor that limits our results is the lack of anatomical validation for the human brain. This is particularly important for the presence of the interhemispheric claustral connections that were described in rats, cats, and primates, but never before in the human brain (Kunzle 1975; Cortimiglia et al. 1991; Smith and Alloway 2010; Park et al. 2012).

Further studies should be obtained from the human brain using postmortem microsurgery dissection and/or tracer injection or in vivo fMRI in order to confirm the existence of this long-range interclaustral pathway.

Conclusion

Despite the described limitations, CSD tractography approach provided an accurate in vivo reconstruction of the complex network of claustrum pathways in the human brain, including details on interhemispheric claustral connections.

From the functional point of view, our findings, in association with results of anatomical and functional studies carried out mainly in animals, confirmed that the claustrum can be considered as a functional bridge among many cortical and subcortical areas of the brain hemispheres.

This complex scenery of claustro-cortical and subcortical connections could play a role in responses to salient stimuli, flowing through multiple cognitive channels, before their externalization.

In clinical setting, the role of claustrum is potentially important and worthy of further and extensive investigations. For instance, since the diffusion of neoplastic cells along the white fiber tracts is well established, extensive claustro-cortical connections are potential pathways of diffusion of high-grade gliomas throughout the entire brain. Consequently, it is necessary to pay attention to this issue in planning surgery, particularly in the presence of insular gliomas invading the claustrum.

Future studies are necessary to clarify the role of claustrum in producing visual hallucinations and other cognitive dysfunctions in patients with DBL, PD, AD, and autism.

Finally, another important and fascinating area of research will be to dissect the role of claustrum in human consciousness.

Notes

Conflict of Interest: None declared.

References

Alexander DC, Barker GJ. 2005. Optimal imaging parameters for fiber-orientation estimation in diffusion MRI. NeuroImage. 27:357–367.

Amaral DG, Cowan WM. 1980. Subcortical afferents to the hippocampal formation in the monkey. J Comp Neurol. 189:573–591.

Amaral DG, Insausti R. 1992. Retrograde transport of D-[3H]-aspartate injected into the monkey amygdaloid complex. Exp Brain Res. 88: 375–388.

Arikuni T, Kubota K. 1985. Claustral and amygdaloid afferents to the head of the caudate nucleus in macaque monkeys. Neurosci Res. 2:239–254.

Babalola KO, Patenaude B, Aljabar P, Schnabel J, Kennedy D, Crum W, Smith S, Cootes T, Jenkinson M, Rueckert D et al. 2009. An evaluation of four automatic methods of segmenting the subcortical structures in the brain. NeuroImage. 47:1435–1447.

Baugh LA, Lawrence JM, Marotta JJ. 2011. Novel claustrum activation observed during a visuomotor adaptation task using a viewing window paradigm. Behav Brain Res. 223:395–402.

Behrens TE, Berg HJ, Jbabdi S, Rushworth MF, Woolrich MW. 2007. Probabilistic diffusion tractography with multiple fibre orientations: what can we gain? NeuroImage. 34:144–155.

Bürger K, Fraedrich R, Merhof D, Westermann R. 2012. Instant visitation maps for interactive visualization of uncertain particle trajectories. Proc SPIE. 8294:1–12.

Calvert GA. 2001. Crossmodal processing in the human brain: insights from functional neuroimaging studies. Cereb Cortex. 11:1110–1123.

Chung HW, Chou MC, Chen CY. 2011. Principles and limitations of computational algorithms in clinical diffusion tensor MR tractography. Am J Neuroradiol. 32:3–13.

Chung SW, Lu Y, Henry RG. 2006. Comparison of bootstrap approaches for estimation of uncertainties of DTI parameters. NeuroImage. 33:531–541.

Cohen-Adad J, Descoteaux M, Wald LL. 2011. Quality assessment of high angular resolution diffusion imaging data using bootstrap on Q-ball reconstruction. J Magn Reson Imaging. 33:1194–1208.

Cortimiglia R, Crescimanno G, Salerno MT, Amato G. 1991. The role of the claustrum in the bilateral control of frontal oculomotor neurons in the cat. Exp Brain Res. 84:471–477.

Crick FC, Koch C. 2005. What is the function of the claustrum? Philos Trans R Soc Lond B Biol Sci. 360:1271–1279.

Davis WB. 2008. The claustrum in autism and typically developing male children: a quantitative MRI study. Brigham: Young University.

Descoteaux M, Deriche R, Knösche TR, Anwander A. 2009. Deterministic and probabilistic tractography based on complex fibre orientation distributions. IEEE Trans Med Imaging. 28:269–286.

Druga R. 1982. Claustro-neocortical connections in the cat and rat demonstrated by HRP tracing technique. J Hirnforsch. 23:191–202.

Duffau H, Mandonnet E, Gatignol P, Capelle L. 2007. Functional compensation of the claustrum: lessons from low-grade glioma surgery. J Neurooncol. 81:327–329.

Edelstein LR, Denaro FJ. 2004. The claustrum: a historical review of its anatomy, physiology, cytochemistry and functional significance. Cell Mol Biol (Noisy-le-Grand). 50:675–702.

Efron B. 1992. Jackknife-after-bootstrap standard errors and influence functions (with discussion). J R Stat Soc Ser B. 54:83–127.

Embleton KV, Haroon HA, Morris DM, Ralph MA, Parker GJ. 2010. Distortion correction for diffusion-weighted MRI tractography and fMRI in the temporal lobes. Hum Brain Mapp. 31:1570–1587.

Fernández-Miranda JC, Rhoton AL Jr, Kakizawa Y, Choi C, Alvarez-Linera J. 2008. The claustrum and its projection system in the human brain: a microsurgical and tractographic anatomical study. J Neurosurg. 108:764–774.

Fortsmann BU, Keuken MC, Jahfari S, Bazin PL, Neumann J, Schafer A, Anwander A, Turner R 2012. Cortico-subthalamic white matter strenght predicts interindividual efficacy in stopping a motor response. NeuroImage. 60:370–375.

Hadjikhani N, Roland PE. 1998. Cross-modal transfer of information between the tactile and the visual representations in the human brain: a positron emission tomographic study. J Neurosci. 18:1072–1084.

Highley JR, Walker MA, Esiri MM, Crow TJ, Harrison PJ. 2002. Asymmetry of the uncinate fasciculus: a post-mortem study of

normal subjects and patients with schizophrenia. Cereb Cortex. 12: 1218–1224.
Jiménez-Castellanos J Jr, Reinoso-Suárez F. 1985. Topographical organization of the afferent connections of the principal ventromedial thalamic nucleus in the cat. J Comp Neurol. 236:297–314.
Joe BN, Fukui MB, Meltzer CC, Huang QS, Day RS. 1999. Brain tumor volume measurement: comparison of manual and semiautomated methods. Radiology. 212:811–816.
Jones DK, Cercignani M. 2010. Twenty-five pitfalls in the analysis of diffusion MRI data. NMR Biomed. 23:803–820.
Jones DK, Horsfield MA, Simmons A. 1999. Optimal strategies for measuring diffusion in anisotropic systems by magnetic resonance imaging. Magn Reson Med. 42:515–525.
Just MA, Cherkassky VL, Keller TA, Kana RK, Minshew NJ. 2007. Functional and anatomical cortical underconnectivity in autism: evidence from an fMRI study of an executive function task and corpus callosum morphometry. Cereb Cortex. 17:951–961.
Kapakin S. 2011. The claustrum: three-dimensional reconstruction, photorealistic imaging, and stereotactic approach. Folia Morphol. 70:228–234.
Kimura S, Nezu A, Osaka H, Saito K. 1994. Symmetrical external capsule lesions in a patient with herpes simplex encephalitis. Neuropediatrics. 25:162–164.
Kosaka K. 1978. Lewy bodies in cerebral cortex, report of three cases. Acta Neuropathol. 42:127–134.
Kunzle H. 1975. Bilateral projections from precentral motor cortex to the putamen and other parts of the basal ganglia. An autoradiographic study in *Macaca fascicularis*. Brain Res. 88:195–209.
Laird AR, Robinson JL, McMillan KM, Tordesillas-Gutierrez D, Moran ST, Gonzales SM, Ray KL, Franklin G, Glahn DC, Fox PT et al. 2010. Comparison of the disparity between Talairach and MNI coordinates in functional neuroimaging data: validation of the Lancaster transform. NeuroImage. 51:677–683.
Leemans A, Jeurissen B, Sijbers J, Jones DK. 2009. ExploreDTI: a graphical toolbox for processing, analyzing, and visualizing diffusion MR data. Proc Intl Soc Mag Reson Med. 17:3536.
Leemans A, Jones DK. 2009. The B-matrix must be rotated when correcting for subject motion in DTI data. Magn Reson Med. 61: 1336–1349.
Lerner A, Bagic A, Hanakawa T, Boudreau EA, Pagan F, Mari Z, Bara-Jimenez W, Aksu M, Sato S, Murphy DL et al. 2009. Involvement of insula and cingulate cortices in control and suppression of natural urges. Cereb Cortex. 19:218–223.
LeVay S, Sherk H. 1981. The visual claustrum of the cat. I. Structure and connections. J Neurosci. 1:956–980.
Martuzzi R, Murray MM, Michel CM, Thiran JP, Maeder PP, Clarke S. 2007. Multisensory interactions within human primary cortices revealed by BOLD dynamics. Cereb Cortex. 17:1672–1679.
Milazzo C, Anastasi G, Bramanti P, Quartarone A, Arrigo A, Giordano A, Azzerboni B, Finocchio G, Milardi D. 2012. A multimodal approach to trace motor cortical-peripheral pathways based on mixed transcranial magnetic stimulation and diffusion tensor imaging technique. Adv Biomed Eng. 14:482–487.
Molholm S, Ritter W, Murray MM, Javitt DC, Schroeder CE, Foxe JJ. 2002. Mutisensory audio–visual interactions during early sensory processing in humans: a high- density electrical mapping study. Brain Res Cogn Brain Res. 14:115–128.
Morys J, Bobinski M, Wegiel J, Wisniewski HM, Narkiewicz O. 1996. Alzheimer's disease severely affects areas of the claustrum connected with the entorhinal cortex. J Hirnforsch. 37:173–180.
Naghavi HR, Eriksson J, Larsson A, Nyberg L. 2007. The claustrum/insula region integrates conceptually related sounds and pictures. Neurosci Lett. 422:77–80.
Nishizawa M. 2005. Acute encephalopathy after ingestion of "sugihiratake" mushroom. Rinsho Shinkeigaku. 45:818–820.
Norita M. 1977. Demonstration of bilateral claustro-cortical connections in the cat with the method of retrograde axonal transport of horseradish peroxidase. Arch Histol Jpn. 40:1–10.
Oldfield RC. 1971. The assessment and analysis of handedness: the Edinburgh inventory. Neuropsychologia. 9:97–113.
Olson CR, Graybiel AM. 1980. Sensory maps in the claustrum of the cat. Nature. 288:479–481.
Pajevic S, Pierpaoli C. 1999. Color schemes to represent the orientation of anisotropic tissues from diffusion tensor data: application to white matter fiber tract mapping in the human brain. Magn Reson Med. 42:526–540.
Park S, Tyszka JM, Allman JM. 2012. The claustrum and insula in *Microcebus murinus*: a high resolution diffusion imaging study. Front Neuroanat. 6:21.
Parker GD, Marshall D, Rosin PL, Drage N, Richmond S, Jones DK. 2013. A pitfall in the reconstruction of fibre ODfs using spherical deconvolution of diffusion MRI data. Neuroimage. 65:433–448.
Pearson RC, Brodal P, Gatter KC, Powell TP. 1982. The organization of the connections between the cortex and the claustrum in the monkey. Brain Res. 234:435–441.
Pedraza O, Bowers D, Gilmore R. 2004. Asymmetry of the hippocampus and amygdala in MRI volumetric measurements of normal adults. J Int Neuropsychol Soc. 10:664–678.
Redouté J, Stoleru S, Gregoire MC, Costes N, Cinotti L, Lavennef F, Le Bars D, Forest MG, Pujol GF. 2000. Brain processing of visual sexual stimuli in human males. Hum Brain Mapp. 11:162–177.
Sherk H, LeVay S. 1981. The visual claustrum of the cat. III. Receptive field properties. J Neurosci. 1:993–1002.
Smiley JF, Falchier A. 2009. Multisensory connections of monkey auditory cerebral cortex. Hear Res. 258:37–46.
Smith JB, Alloway KD. 2010. Functional specificity of claustrum connections in the rat: interhemispheric communication between specific parts of motor cortex. J Neurosci. 30:16832–16844.
Smythies J, Edelstein L, Ramachandran V. 2012. Hypotheses relating to the function of the claustrum. Front Integr Neurosci. 6:53.
Sperner J, Sander B, Lau S, Krude H, Scheffner D. 1996. Severe transitory encephalopathy with reversible lesions of the claustrum. Pediatr Radiol. 26:769–771.
Stevens CF. 2005. Consciousness: crick and the claustrum. Nature. 435: 1040–1041.
Tanné-Gariépy J, Boussaoud D, Rouiller EM. 2002. Projections of the claustrum to the primary motor, premotor, and prefrontal cortices in the macaque monkey. J Comp Neurol. 454:140–157.
Thiebaut de Schotten M, Ffytche DH, Bizzi A. 2011. Atlasing location, asymmetry and intersubject variability of white matter tracts in the human brain with diffusion tractography. Neuroimage. 54:49–59.
Tournier JD, Calamante F, Connelly A. 2011. Effect of step size on probabilistic streamlines: implications for the interpretation of connectivity analysis. Proc Intl Soc Mag Reson Med. 19:2019.
Tournier JD, Calamante F, Connelly A. 2007. Robust determination of the fibre orientation distribution in diffusion MRI: non-negativity constrained super-resolved spherical deconvolution. Neuroimage. 35:1459–1472.
Tournier JD, Yeh CH, Calamante F, Cho KH, Connelly A, Lin CP. 2008. Resolving crossing fibres using constrained spherical deconvolution: validation using diffusion-weighted imaging phantom data. Neuroimage. 42:617–625.
Ture U, Yasargil MG, Friedman AH, Al-Mefty O. 2000. Fiber dissection technique: lateral aspect of the brain. Neurosurgery. 47:417–426.
Uhlhaas PJ, Pipa G, Lima B, Melloni L, Neuenschwander S, Nikolić D, Singer W. 2009. Neural synchrony in cortical networks: history, concept and current status. Front Integr Neurosci. 3:17.
Verstynen T, Jarbo K, Pathak S, Schneider W. 2011. In vivo mapping of microstructural somatotopies in the human corticospinal pathways. J Neurophysiol. 105:336–346.
Yamamoto R, Iseki E, Murayama N, Minegishi M, Marui W, Togo T, Katsuse O, Kosaka K, Kato M, Iwatsubo T et al. 2007. Correlation in Lewy pathology between the claustrum and visual areas in brains of dementia with Lewy bodies. Neurosci Lett. 415:219–224.
Zhou YD, Ardestani A, Fuster JM. 2007. Distributed and associative working memory. Cereb Cortex. 17:i77–i87.